ATOM PROBE CHARACTERIZATION OF PREPRECIPITATE CLUSTERS AND PRECIPITATES IN Al-Mg-Si(-Cu) ALLOYS

M. MURAYAMA and K. HONO

National Research Institute for Metals, 1-2-1 Sengen, Tsukuba 305-0047, Japan

ABSTRACT Pre-precipitation clustering and chemical nature of the metastable precipitates in aged Al-Mg-Si(-Cu) alloys have been investigated by atom probe field ion microscopy (APFIM) and transmission electron microscopy (TEM) for better understanding of the two-step aging behavior and the effect of excess Si. After a prolonged natural aging, co-clusters of Mg and Si atoms are observed in addition to separate Si- and Mg- clusters. The ratio of Mg to Si atoms in the co-clusters is approximately 1:1. Spherical G.P. zones are present after pre-aging for 16 h at 70°C, and they contain 20 at.% Mg and 20 at.%Ag. The density of the β″ that precipitates after 30 min aging at 175°C increases significantly when the specimen is pre-aged at 70°C, suggesting that G.P. zones formed at 70°C serve as nucleation sites for the β″ in the subsequent 175°C aging. On the other hand, co-clusters formed at room temperature do not serve as nucleation sites for the β″ precipitates. The mechanism of adverse artificial age hardening response after natural aging is discussed.

Keywords: *precipitation, Al-Mg-Si alloy, β" phase, G.P. zone, two-step aging*

1. INTRODUCTION

In the continuing drive for automobile weight reduction, Al-Mg-Si(-Cu) alloys are considered to be the most promising candidates for heat treatable bodysheet materials. Several studies [1-3] reported that alloys containing an excess amount of Si above the Al-Mg_2Si quasi-binary composition show pronounced hardening by aging at 175 °C. However such hardening response is significantly suppressed when the specimen receives a room temperature aging for a prolonged period of time. Since the natural aging after a solution heat treatment can not be avoided in the automobile manufacturing process, understanding of the mechanism of this adverse age hardening effect is strongly desired.

The precipitation process of Al-Mg-Si alloys have been a subject of numerous studies. The most likely precipitation sequence [4] is

solute clusters → G. P. zones (spherical) → β″ (needle) → β″ (rod).

The formation of Si clusters was predicted based on the DSC measurement results [4], and subsequently, Edwards et al. [5] found direct evidence for separate Si- and Mg-clusters and Si-Mg co-clusters during aging at 70°C using the atom probe field ion microscope (APFIM) technique. In their study, however, solute clustering during natural aging was not investigated. Characterizing features of possible solute clusters during natural aging is extremely important in order to understand the mechanism how room temperature aging causes adverse age hardening response in artificial aging at 175°C. It is also important to determine the chemical composition of above mentioned solute clusters and precipitation products, in order to understand the effect of Si content on the age hardening response. However, the chemical compositions of G.P. zones, β" and β' precipitates in this alloy system are still elusive [6], because conventional analytical techniques do not have sufficient spatial resolution to measure the chemical composition of such small objects embedded in the matrix phase with high accuracy.

This study aimed to obtain better understanding of the mechanism of adverse age hardening effect due to natural aging and the role of excess amount of Si on changing the age hardening response. For this purpose, we attempted to clarify the chemical natures of various precipitation products in Al-Mg-Si(-Cu) alloys which form after natural aging, pre-aging at 70°C, and artificial aging at 175°C by a conventional atom probe (AP), a three dimensional atom probe (3DAP) and transmission electron microscope (TEM). Employment of 3DAP is particularly effective, because of its capability of mapping individual atoms in the real space with a near-atomic resolution [7,8], and thus it reveals information on the density and the morphology of clusters and small precipitates. In addition, 3DAP has improved accuracy in determining chemical composition of small precipitates, because atoms for

determining composition can be collected only from within a precipitate without any convolution artifact.

2. EXPERIMENTAL

Chemical compositions of the alloys used in this study are listed in Table 1. These alloys were solution treated at 550 °C for 30 min and subsequently water quenched. The solution treated samples were subjected to various heat treatments including natural aging for 70 days, pre-aging for 16 h at 70 °C, artificial aging for 10 h at 175 °C and artificial aging after the pre-aging (two-step aging). For atom probe analyses, an energy compensated time-of-flight atom probe (AP) and a three.dimensional atom probe (3DAP) equipped with CAMECA's tomographic atom probe (TAP) detection system [8] were used. Field ion microscopy images were observed at temperatures of 20 - 30 K with He as an imaging gas, and atom probe analyses were carried out at about 30 K with a pulse fraction (V_p/V_{dc}) of 20% in UHV (~$1x10^{-10}$ Torr). Microstructures of the samples were examined with a transmission electron microscope (TEM), Philips CM200, operated at 200 kV.

Table 1 Chemical compositions of the alloys (at. %)

Alloy	Mg	Si	Cu	Fe	Ti	Al
Balance	0.70	0.33	-	0.024	0.006	bal.
Si-excess	0.65	0.70	-	0.005	-	bal.
Cu-added	0.61	1.22	0.38	0.05	-	bal.

3. RESULTS AND DISCUSSION

Figure 1 (a) - (e) show TEM bright field images and the [001] selected area diffraction pattern (SADP) obtained from the Si-excess alloy with various aging conditions. In the case of the naturally aged specimen (Fig. 1(a)), no indication of the presence of precipitates are recognized. On the other hand, the specimen aged at 70°C for 16 h shows a contrast arising from extremely fine precipitates (Fig. 1(b)). However, the shape of the fine precipitates is unresolved, and the SADP show neither extra reflections nor diffuse scattering. This suggests that the precipitates are fully coherent and the aspect ratio of these particles is close to 1, thus the precipitates are characterized as spherical G.P. zones as reported by Dutta and Allen [4]. The specimens shown in Figs. 1 (c-d) were all aged at 175 °C for 3 h after various previous conditions, i.e., (c) right after a solution heat treatment, (d) after natural aging and (e) after a pre-aging at 70 °C for 16 h. Each of the images show strain field contrast

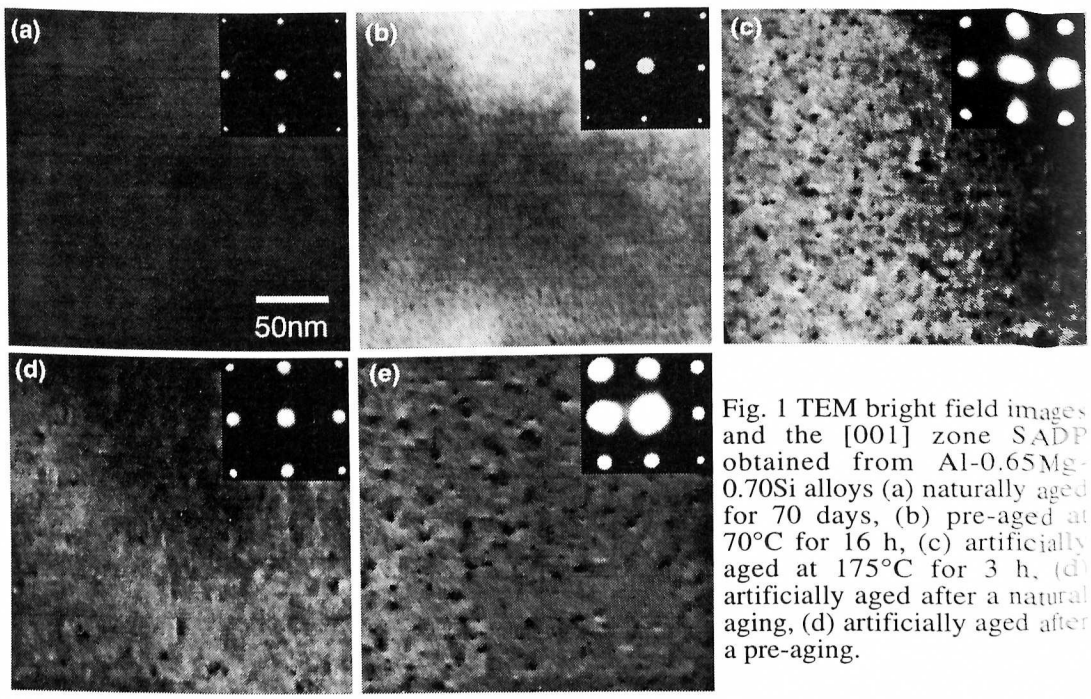

Fig. 1 TEM bright field images and the [001] zone SADP obtained from Al-0.65Mg-0.70Si alloys (a) naturally aged for 70 days, (b) pre-aged at 70°C for 16 h, (c) artificially aged at 175°C for 3 h, (d) artificially aged after a natural aging, (d) artificially aged after a pre-aging.

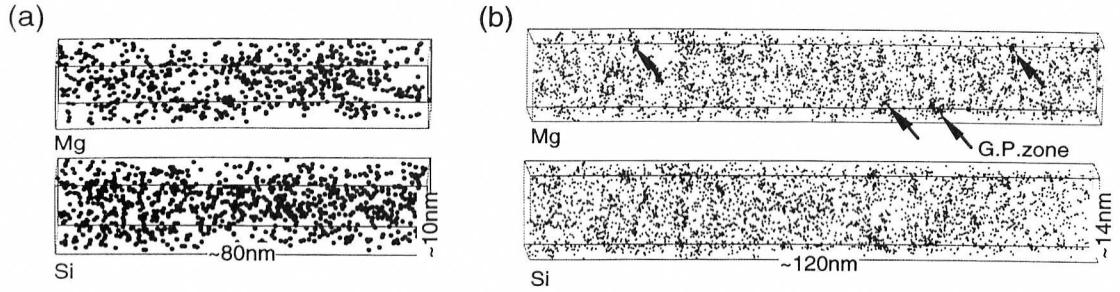

Figures 2 3DAP elemental mappings of Mg and Si obtained from the Si-excess specimens which were subjected to (a) a prolonged natural aging and (b) a pre-aging at 70°C for 16 h. Spherical G.P. zones are observed (arrow).

from needle-shape precipitates. The specimen artificially aged after the 70°C pre-aging has the highest density of the needle-shape precipitates. The streaks along the <100> directions have characteristic feature consistent with the β″ precipitates [9]. The density of the β″ precipitates is somewhat lower in the specimen artificially aged right after the solution treatment, and the lowest density is observed in the specimen artificially aged after the natural aging. These observations suggest that the G.P. zones formed during the 70°C pre-aging somehow increased the density of nuclei for precipitation of the β″, while natural aging reduces nucleation density or precipitation kinetics in the subsequent artificial aging process.

Figures 2 (a) and (b) show 3DAP elemental mappings of Mg and Si obtained from the Si-excess specimens which were subjected to (a) prolonged natural aging and (b) pre-aging at 70°C for 16 h. In the naturally aged specimen, the distribution of Si and Mg atoms appears to be homogeneous at a glance. Since the concentration of Si and Mg is in a few atomic percent level and these give relatively high background, small clustering cannot be visualized from the raw data. Thus, a statistical method known as contingency table analysis was employed to test whether or not there is a correlation in distributions of Ag and Mg atoms. Table 2 (a) shows contingency tables of the number of Mg and Si atoms based on a block size of 146 atoms for the naturally aged specimen. In this table, observed frequencies containing categorized numbers of Mg and Si atoms are tabulated. Experimentally observed frequencies and the frequencies estimated for random distribution of Mg and Si are

Table. 2 Contingency tables for Mg and Si

(a) natural aged specimen

		Observed						Expected				
		Si						Si				
		0	1	2	≥3	Total		0	1	2	≥3	Total
Mg	0	175	60	25	19	279	0	143.7	70.9	36.6	27.8	279
	1	120	69	36	19	244	1	125.7	62.0	32.0	24.3	244
	2	66	40	23	24	153	2	78.8	38.9	20.1	15.2	153
	≥3	32	25	16	14	87	≥3	44.8	22.1	11.4	8.7	87
	Total	393	194	100	76	763	Total	393	194	100	76	763

$\chi^2 = 34.396$ with 9 degrees of freedom

(b) 70 °C pre-aged specimen

		Observed						Expected				
		Si						Si				
		0	1	2	≥3	Total		0	1	2	≥3	Total
Mg	0	406	224	87	40	757	0	332.9	236.6	104.8	82.7	757
	1	247	191	82	51	571	1	251.1	178.5	79.1	62.4	571
	2	109	102	34	41	286	2	125.8	89.4	39.6	31.2	286
	3	30	39	31	32	132	3	58.0	41.3	18.3	14.4	132
	4	15	10	10	15	50	4	22.0	15.6	6.9	5.5	50
	≥5	6	12	12	23	53	≥5	23.3	16.6	7.3	5.8	53
	Total	812	578	256	202	1894	Total	813	578	256	202	1894

$\chi^2 = 187.245$ with 15 degrees of freedom

compared using the χ^2 test. The calculated value of χ^2 is 34.4 with 9 degrees of freedom, thus the null hypothesis that there is no correlation between Mg and Si atoms is rejected with a significance level of 99.999 % ($\alpha < 0.001$). The table also suggests that there is a positive correlation between Si and Mg atoms, thus it can be concluded that Si and Mg co-clusters are present in the naturally aged specimen.

In the 70°C pre-aged specimen, presence of spherical clusters enriched with Si and Mg atoms is evident from the elemental mappings (Fig. 2 (b)). The shape of the Si and Mg aggregates are spherical, thus these are believed to correspond with the spherical G.P. zones characterized by TEM in Fig. 1 (b). The contingency table test (Table 2 (b)) shows more convincingly that there is strong correlation between Mg and Si atoms (χ^2 value is 187 with 15 degrees of freedom). The chemical composition of these G.P. zones has been determined to be 20 at.%Mg and 20 at.%Si by careful analysis of 3DAP data.

Although the 3DAP elemental mapping does not demonstrate visually the presence of solute clusters, local concentration changes can be detected more sensitively by analyzing the data obtained by conventional atom probe. Figure 3 shows integrated concentration depth profiles, or ladder plot, of the naturally aged Si-excess alloy. In these diagrams, the number of detected solute atoms are plotted as a function of the total number of detected atoms. Thus, the slope of the plots represents the local concentration of the alloy and the horizontal axis corresponds to the depth. Steep changes in the slope are recognized (indicated by arrowheads) in both Mg and Si ladder diagram. In these regions, concentration of Mg or Si is significantly higher than the average concentration in the alloy, suggesting that there are separate clusters of Mg and Si atoms (indicated by arrows). In addition, co-clusters of Si and Mg atoms are observed, and the ratio of the number of Si and Mg atoms are close to 1.

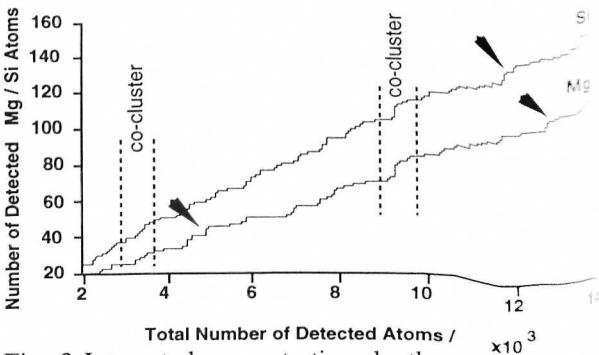

Fig. 3 Integrated concentration depth profiles of A 0.65Mg-0.70Si after a natural aging for 70 days. I addition to separate clusters of Mg and S (arrowheads), co-clusters of Mg and Si atoms a observed (dushed line).

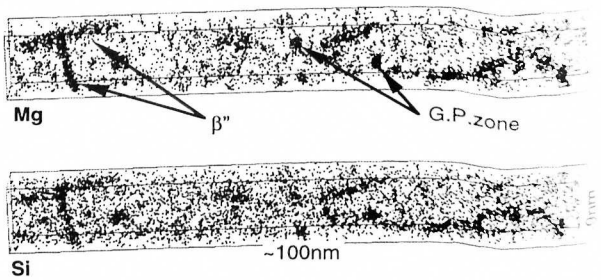

Fig. 4 3DAP elemental mappings of Mg and S obtained from the Si-excess alloy aged at 175 °C f 10 h after a pre-aging at 70°C.

Based on these AP observations, it can be concluded that Mg and Si atoms aggregate each oth and form either co-clusters or G.P. zones during pre-aging. Both are similar in chemistry, but G zones are lager than clusters and they are observable by TEM, thus G.P. zones are expected to b more stable than co-clusters. As pre-aging at 70°C increases the number density of β″ precipitat produced during artificial aging at 175°C, we believe that some of the G.P. zones serve as nucleati sites for β″ precipitates. On the other hand, co-clusters formed during natural aging are so small a unstable that they dissolve at the temperature of artificial aging and they do not provide any nucleati site for β″. When co-clusters are reverted, kinetics for precipitation become slower, because most the quenched-in vacancies disappear and the vacancy concentration reach the equilibrium value at t reversion temperature. In addition, the driving force for precipitation with low undercooling from t solvus (at a higher aging temperature) is lower. Thus the present observation is consistent with th well know mechanism for two-step aging proposed by Lorimer and Nicholson [10].

Figure 4 shows 3DAP elemental mappings of Mg and Si obtained from the Si-excess alloy whi was artificially aged at 175 °C for 10 h after pre-aging at 70°C. Needle-shape precipitates and spheri G.P. zones are observed. The needle-shape precipitates are composed of Mg and Si atoms, and th composition is approximately 23%Mg and 21%Si, which is very close to that of the spherical G zones observed after the 70°C pre-aging. The needle-shape precipitates are believed to be β" based the SADP shown in Fig. 1(d). Because the β" precipitates have a similar chemical composition to th

G.P. zones which are formed at the pre-aging stage, it is likely that G.P. zones can serve as nucleation sites or they can evolve to β" in the subsequent aging. Comparison with the chemical composition of the β″ in the balanced alloy is of particular interest in order to understand the role of excess Si; unfortunately, it has not been determined so far, because the density of the β″ precipitates in the balanced alloy was too low to be detected by the AP technique. Further study to compare the chemical compositions of the β″ precipitates in the alloys with different Si concentrations is in progress. Considering the mass balance of the solutes, composition of the precipitates in the balanced alloy should be close to that of Mg_2Si, otherwise excess Mg must form different precipitate or clusters. So far, different type or precipitates or clusters composed of only Mg have not been detected.

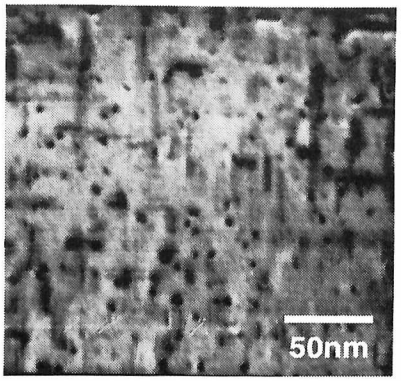

Fig. 5 TEM bright field image of Al-0.70Mg-0.33Si aged at 175°C for 10 h. followed by pre-aging at 70°C for 16 h.

Figure 5 shows a bright field TEM image obtained from the balanced alloy aged at 175 °C for 10 h after 70°C pre-aging. In the bright field image, the needle-shape strain field contrast which arises from the β" precipitates are observed. However, the coarsely distributed larger precipitates indicate that the nucleation of the β" precipitates in the balanced alloy is not so much stimulated by the pre-aging. It is, thus, reasonable to conclude that the excess Si provides much opportunity for the β" precipitates to nucleate at the early stage of aging. This may suggest that the size and density of the G.P. zones formed during the pre-aging stage is much smaller in the balanced alloy. For a better understanding of the role of excess Si, further characterization of clusters formed at the pre-aging stage in the balanced alloy is necessary.

Figure 6 shows 3DAP elemental mapping of Mg, Si and Cu obtained from the Al-0.6Mg-1.2Si-0.4Cu quaternary alloy which was artificially aged at 175 °C for 10 h after 70°C pre-aging. In this specimen, needle-shape β" precipitates and spherical G.P. zones are observed. The composition of the β" precipitates has been determined to be approximately 16 at.% Mg, 13 at.% Si and 4 at.% Cu. Therefore, we can conclude that Cu is incorporated in the β" precipitates. It should be noted that there is no enrichment of Cu in the spherical particles, suggesting that Cu is partitioned only in the needle-shape β" precipitates. In Cu containing quaternary alloys, the equilibrium Q phase ($Al_5Cu_2Mg_8Si_6$) [11] and its precursor phase, Q', was reported [12-14]. In the present study, we have not detected these quaternary phases so far, and characterization of these phases is a subject of further study.

CONCLUSIONS

Solute clustering, formation of G.P. zones and precipitation of the β" precipitates have been studied by APFIM. After a prolonged natural aging, separate Mg- and Si-clusters and their co-clusters are present. The co-clusters are chemically similar to the spherical G.P. zones which are formed after 16 h aging at 70 °C. Increase in density of β" precipitates by artificial aging after pre-aging suggests that some of the G.P. zones serve as nucleation sites for the β" precipitates. On the other hand, decrease in density of β" precipitates after natural aging indicate that co-clusters are reverted at the temperature of artificial aging, resulting in reduced kinetics of further precipitation. The excess amount of Si may provide more opportunity to form

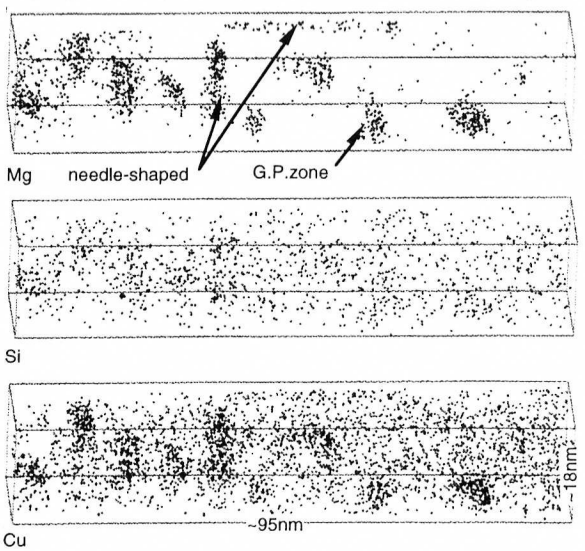

Fig. 6 3DAP elemental mapping of Mg, Si and Cu obtained from the addition of Cu alloy aged at 175°C for 10 h after pre-aging.

compared using the χ^2 test. The calculated value of χ^2 is 34.4 with 9 degrees of freedom, thus the null hypothesis that there is no correlation between Mg and Si atoms is rejected with a significance level of 99.999 % ($\alpha < 0.001$). The table also suggests that there is a positive correlation between Si and Mg atoms, thus it can be concluded that Si and Mg co-clusters are present in the naturally aged specimen.

In the 70°C pre-aged specimen, presence of spherical clusters enriched with Si and Mg atoms is evident from the elemental mappings (Fig. 2 (b)). The shape of the Si and Mg aggregates are spherical, thus these are believed to correspond with the spherical G.P. zones characterized by TEM in Fig. 1 (b). The contingency table test (Table 2 (b)) shows more convincingly that there is strong correlation between Mg and Si atoms (χ^2 value is 187 with 15 degrees of freedom). The chemical composition of these G.P. zones has been determined to be 20 at.%Mg and 20 at.%Si by careful analysis of 3DAP data.

Although the 3DAP elemental mapping does not demonstrate visually the presence of solute clusters, local concentration changes can be detected more sensitively by analyzing the data obtained by conventional atom probe. Figure 3 shows integrated concentration depth profiles, or ladder plot, of the naturally aged Si-excess alloy. In these diagrams, the number of detected solute atoms are plotted as a function of the total number of detected atoms. Thus, the slope of the plots represents the local concentration of the alloy, and the horizontal axis corresponds to the depth. Steep changes in the slope are recognized (indicated by arrowheads) in both Mg and Si ladder diagram. In these regions, concentration of Mg or Si is significantly higher than the average concentration in the alloy, suggesting that there are separate clusters of Mg and Si atoms (indicated by arrows). In addition, co-clusters of Si and Mg atoms is observed, and the ratio of the number of Si and Mg atoms are close to 1.

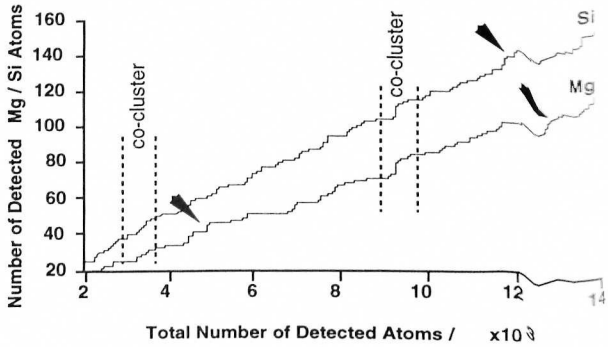

Fig. 3 Integrated concentration depth profiles of Al-0.65Mg-0.70Si after a natural aging for 70 days. In addition to separate clusters of Mg and Si (arrowheads), co-clusters of Mg and Si atoms are observed (dushed line).

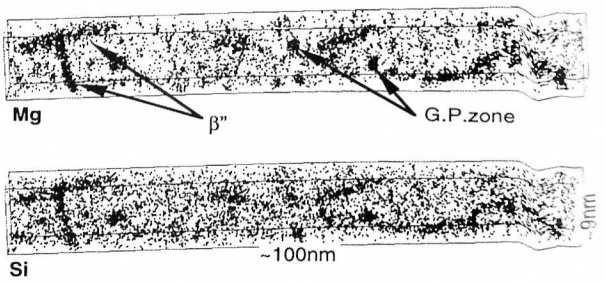

Fig. 4 3DAP elemental mappings of Mg and Si obtained from the Si-excess alloy aged at 175 °C for 10 h after a pre-aging at 70°C.

Based on these AP observations, it can be concluded that Mg and Si atoms aggregate each other and form either co-clusters or G.P. zones during pre-aging. Both are similar in chemistry, but G.P. zones are lager than clusters and they are observable by TEM, thus G.P. zones are expected to be more stable than co-clusters. As pre-aging at 70°C increases the number density of β″ precipitates produced during artificial aging at 175°C, we believe that some of the G.P. zones serve as nucleation sites for β″ precipitates. On the other hand, co-clusters formed during natural aging are so small and unstable that they dissolve at the temperature of artificial aging and they do not provide any nucleation site for β″. When co-clusters are reverted, kinetics for precipitation become slower, because most of the quenched-in vacancies disappear and the vacancy concentration reach the equilibrium value at the reversion temperature. In addition, the driving force for precipitation with low undercooling from the solvus (at a higher aging temperature) is lower. Thus the present observation is consistent with the well know mechanism for two-step aging proposed by Lorimer and Nicholson [10].

Figure 4 shows 3DAP elemental mappings of Mg and Si obtained from the Si-excess alloy which was artificially aged at 175 °C for 10 h after pre-aging at 70°C. Needle-shape precipitates and spherical G.P. zones are observed. The needle-shape precipitates are composed of Mg and Si atoms, and their composition is approximately 23%Mg and 21%Si, which is very close to that of the spherical G.P. zones observed after the 70°C pre-aging. The needle-shape precipitates are believed to be β" based on the SADP shown in Fig. 1(d). Because the β" precipitates have a similar chemical composition to the

G.P. zones which are formed at the pre-aging stage, it is likely that G.P. zones can serve as nucleation sites or they can evolve to β" in the subsequent aging. Comparison with the chemical composition of the β″ in the balanced alloy is of particular interest in order to understand the role of excess Si; unfortunately, it has not been determined so far, because the density of the β″ precipitates in the balanced alloy was too low to be detected by the AP technique. Further study to compare the chemical compositions of the β″ precipitates in the alloys with different Si concentrations is in progress. Considering the mass balance of the solutes, composition of the precipitates in the balanced alloy should be close to that of Mg_2Si, otherwise excess Mg must form different precipitate or clusters. So far, different type or precipitates or clusters composed of only Mg have not been detected.

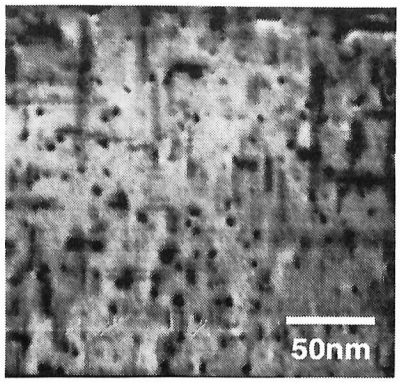

Fig. 5 TEM bright field image of Al-0.70Mg-0.33Si aged at 175°C for 10 h. followed by pre-aging at 70°C for 16 h.

Figure 5 shows a bright field TEM image obtained from the balanced alloy aged at 175 °C for 10 h after 70°C pre-aging. In the bright field image, the needle-shape strain field contrast which arises from the β" precipitates are observed. However, the coarsely distributed larger precipitates indicate that the nucleation of the β" precipitates in the balanced alloy is not so much stimulated by the pre-aging. It is, thus, reasonable to conclude that the excess Si provides much opportunity for the β" precipitates to nucleate at the early stage of aging. This may suggest that the size and density of the G.P. zones formed during the pre-aging stage is much smaller in the balanced alloy. For a better understanding of the role of excess Si, further characterization of clusters formed at the pre-aging stage in the balanced alloy is necessary.

Figure 6 shows 3DAP elemental mapping of Mg, Si and Cu obtained from the Al-0.6Mg-1.2Si-0.4Cu quaternary alloy which was artificially aged at 175 °C for 10 h after 70°C pre-aging. In this specimen, needle-shape β" precipitates and spherical G.P. zones are observed. The composition of the β" precipitates has been determined to be approximately 16 at.% Mg, 13 at.% Si and 4 at.% Cu. Therefore, we can conclude that Cu is incorporated in the β" precipitates. It should be noted that there is no enrichment of Cu in the spherical particles, suggesting that Cu is partitioned only in the needle-shape β" precipitates. In Cu containing quaternary alloys, the equilibrium Q phase ($Al_5Cu_2Mg_8Si_6$) [11] and its precursor phase, Q', was reported [12-14]. In the present study, we have not detected these quaternary phases so far, and characterization of these phases is a subject of further study.

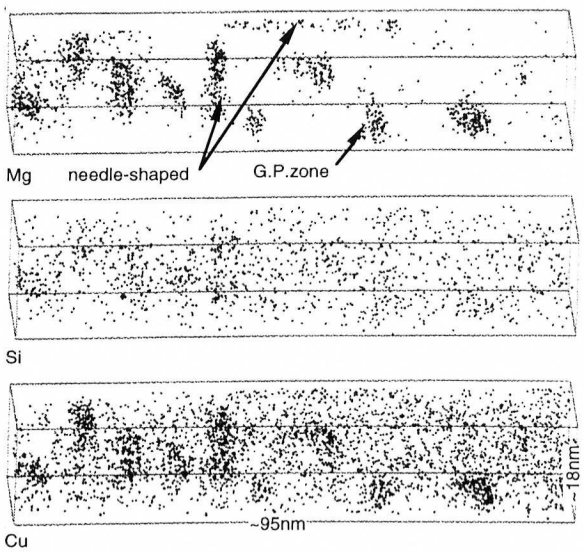

Fig. 6 3DAP elemental mapping of Mg, Si and Cu obtained from the addition of Cu alloy aged at 175°C for 10 h after pre-aging.

CONCLUSIONS

Solute clustering, formation of G.P. zones and precipitation of the β" precipitates have been studied by APFIM. After a prolonged natural aging, separate Mg- and Si-clusters and their co-clusters are present. The co-clusters are chemically similar to the spherical G.P. zones which are formed after 16 h aging at 70 °C. Increase in density of β" precipitates by artificial aging after pre-aging suggests that some of the G.P. zones serve as nucleation sites for the β" precipitates. On the other hand, decrease in density of β" precipitates after natural aging indicate that co-clusters are reverted at the temperature of artificial aging, resulting in reduced kinetics of further precipitation. The excess amount of Si may provide more opportunity to form

compared using the χ^2 test. The calculated value of χ^2 is 34.4 with 9 degrees of freedom, thus the null hypothesis that there is no correlation between Mg and Si atoms is rejected with a significance level of 99.999 % ($\alpha < 0.001$). The table also suggests that there is a positive correlation between Si and Mg atoms, thus it can be concluded that Si and Mg co-clusters are present in the naturally aged specimen.

In the 70°C pre-aged specimen, presence of spherical clusters enriched with Si and Mg atoms is evident from the elemental mappings (Fig. 2 (b)). The shape of the Si and Mg aggregates are spherical, thus these are believed to correspond with the spherical G.P. zones characterized by TEM in Fig. 1 (b). The contingency table test (Table 2 (b)) shows more convincingly that there is strong correlation between Mg and Si atoms (χ^2 value is 187 with 15 degrees of freedom). The chemical composition of these G.P. zones has been determined to be 20 at.%Mg and 20 at.%Si by careful analysis of 3DAP data.

Although the 3DAP elemental mapping does not demonstrate visually the presence of solute clusters, local concentration changes can be detected more sensitively by analyzing the data obtained by conventional atom probe. Figure 3 shows integrated concentration depth profiles, or ladder plot, of the naturally aged Si-excess alloy. In these diagrams, the number of detected solute atoms are plotted as a function of the total number of detected atoms. Thus, the slope of the plots represents the local concentration of the alloy, and the horizontal axis corresponds to the depth. Steep changes in the slope are recognized (indicated by arrowheads) in both Mg and Si ladder diagram. In these regions, concentration of Mg or Si is significantly higher than the average concentration in the alloy, suggesting that there are separate clusters of Mg and Si atoms (indicated by arrows). In addition, co-clusters of Si and Mg atoms is observed, and the ratio of the number of Si and Mg atoms are close to 1.

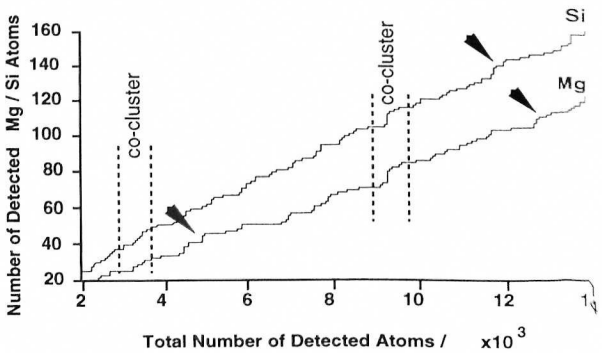

Fig. 3 Integrated concentration depth profiles of Al-0.65Mg-0.70Si after a natural aging for 70 days. In addition to separate clusters of Mg and Si (arrowheads), co-clusters of Mg and Si atoms are observed (dushed line).

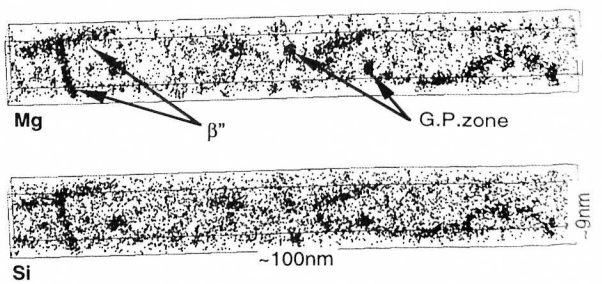

Fig. 4 3DAP elemental mappings of Mg and Si obtained from the Si-excess alloy aged at 175 °C for 10 h after a pre-aging at 70°C.

Based on these AP observations, it can be concluded that Mg and Si atoms aggregate each other and form either co-clusters or G.P. zones during pre-aging. Both are similar in chemistry, but G.P. zones are lager than clusters and they are observable by TEM, thus G.P. zones are expected to be more stable than co-clusters. As pre-aging at 70°C increases the number density of β″ precipitates produced during artificial aging at 175°C, we believe that some of the G.P. zones serve as nucleation sites for β″ precipitates. On the other hand, co-clusters formed during natural aging are so small and unstable that they dissolve at the temperature of artificial aging and they do not provide any nucleation site for β″. When co-clusters are reverted, kinetics for precipitation become slower, because most of the quenched-in vacancies disappear and the vacancy concentration reach the equilibrium value at the reversion temperature. In addition, the driving force for precipitation with low undercooling from the solvus (at a higher aging temperature) is lower. Thus the present observation is consistent with the well know mechanism for two-step aging proposed by Lorimer and Nicholson [10].

Figure 4 shows 3DAP elemental mappings of Mg and Si obtained from the Si-excess alloy which was artificially aged at 175 °C for 10 h after pre-aging at 70°C. Needle-shape precipitates and spherical G.P. zones are observed. The needle-shape precipitates are composed of Mg and Si atoms, and their composition is approximately 23%Mg and 21%Si, which is very close to that of the spherical G.P. zones observed after the 70°C pre-aging. The needle-shape precipitates are believed to be β" based on the SADP shown in Fig. 1(d). Because the β" precipitates have a similar chemical composition to the

G.P. zones which are formed at the pre-aging stage, it is likely that G.P. zones can serve as nucleation sites or they can evolve to β" in the subsequent aging. Comparison with the chemical composition of the β″ in the balanced alloy is of particular interest in order to understand the role of excess Si; unfortunately, it has not been determined so far, because the density of the β″ precipitates in the balanced alloy was too low to be detected by the AP technique. Further study to compare the chemical compositions of the β″ precipitates in the alloys with different Si concentrations is in progress. Considering the mass balance of the solutes, composition of the precipitates in the balanced alloy should be close to that of Mg_2Si, otherwise excess Mg must form different precipitate or clusters. So far, different type or precipitates or clusters composed of only Mg have not been detected.

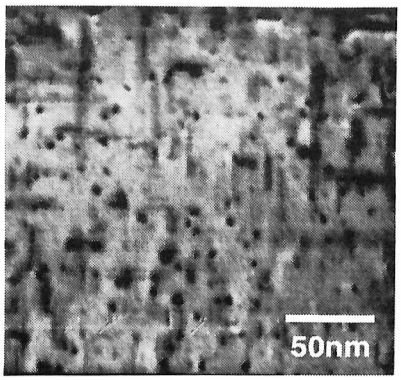

Fig. 5 TEM bright field image of Al-0.70Mg-0.33Si aged at 175°C for 10 h. followed by pre-aging at 70°C for 16 h.

Figure 5 shows a bright field TEM image obtained from the balanced alloy aged at 175 °C for 10 h after 70°C pre-aging. In the bright field image, the needle-shape strain field contrast which arises from the β" precipitates are observed. However, the coarsely distributed larger precipitates indicate that the nucleation of the β" precipitates in the balanced alloy is not so much stimulated by the pre-aging. It is, thus, reasonable to conclude that the excess Si provides much opportunity for the β" precipitates to nucleate at the early stage of aging. This may suggest that the size and density of the G.P. zones formed during the pre-aging stage is much smaller in the balanced alloy. For a better understanding of the role of excess Si, further characterization of clusters formed at the pre-aging stage in the balanced alloy is necessary.

Figure 6 shows 3DAP elemental mapping of Mg, Si and Cu obtained from the Al-0.6Mg-1.2Si-0.4Cu quaternary alloy which was artificially aged at 175 °C for 10 h after 70°C pre-aging. In this specimen, needle-shape β" precipitates and spherical G.P. zones are observed. The composition of the β" precipitates has been determined to be approximately 16 at.% Mg, 13 at.% Si and 4 at.% Cu. Therefore, we can conclude that Cu is incorporated in the β" precipitates. It should be noted that there is no enrichment of Cu in the spherical particles, suggesting that Cu is partitioned only in the needle-shape β" precipitates. In Cu containing quaternary alloys, the equilibrium Q phase ($Al_5Cu_2Mg_8Si_6$) [11] and its precursor phase, Q', was reported [12-14]. In the present study, we have not detected these quaternary phases so far, and characterization of these phases is a subject of further study.

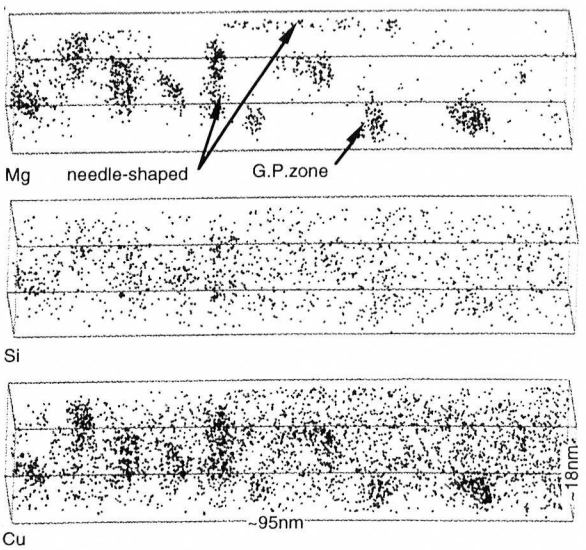

Fig. 6 3DAP elemental mapping of Mg, Si and Cu obtained from the addition of Cu alloy aged at 175°C for 10 h after pre-aging.

CONCLUSIONS

Solute clustering, formation of G.P. zones and precipitation of the β" precipitates have been studied by APFIM. After a prolonged natural aging, separate Mg- and Si-clusters and their co-clusters are present. The co-clusters are chemically similar to the spherical G.P. zones which are formed after 16 h aging at 70 °C. Increase in density of β" precipitates by artificial aging after pre-aging suggests that some of the G.P. zones serve as nucleation sites for the β" precipitates. On the other hand, decrease in density of β" precipitates after natural aging indicate that co-clusters are reverted at the temperature of artificial aging, resulting in reduced kinetics of further precipitation. The excess amount of Si may provide more opportunity to form

G.P. zones in early stage of aging. This leads a high density of β" precipitates.

ACKNOWLEDGMENT

The authors thank Dr. Saga, Nippon Steel Corporation and Professor D. E. Laughlin, Carnegie Mellon University, for provision of specimens used in the present study.

REFERENCES

[1] D.W. Pashley, J.W. Rhodes and A. Sendorek, J. Inst. Metals, 41 (1966), 94.
[2] D.W. Pashley, M.H. Jacobs and J.T. Vietz, Phil. Mag., 51 (1967), 16.
[3] N. Hashimoto, M. Saga, M. Kikuchi, R. Uemori and N. Maruyama, unpublished research. Nippon Steel Co., 1994.
[4] I. Dutta and S.M. Allen, J. Mater. Sci. Lett., 10 (1991), 323.
[5] G.A. Edwards, K. Stiller and G.L. Dunlop, Appl. Surf. Sci., 76/77 (1994), 219.
[6] G.A. Edwards, K. Stiller, G.L. Dunlop and M.J. Couper, Mater. Sci. Forum, 217-222 (1996), 713.
[7] A. Cerezo, T. J. Godfrey and G. D. W. Smith, Rev. Sci. Instrum. 59 (1988), 862.
[8] D. Blavette, B. Deconihout, A. Bostel, J. M. Sarrau, M. Bouet and A. Menand, Rev. Sci. Instrum, 64 (1993), 2911.
[9] J. P. Lynch, L. M. Brown and M. H. Jacobs, Acta metall. 30 (1982), 1389.
[10] G. W. Lorimer and R. B. Nicholson, The Mechanism of Phase Transformations in Crystalline Solids, 1969, The Institute of Metals, London, pp. 36.
[11] D.J. Chakrabarti and J.L. Murray, Mater. Sci. Forum, 217-222 (1996), 177.
[12] A.K. Gupta, P.H. Marois and D.J. Lloyd, Mater. Sci. Forum, 217-222 (1996) 801.
[13] S.D. Dumolt, D.E. Laughlin and J.C. Williams, Scripta Met., 18 (1984), 1347.